PREPARING THE INITIAL MODEL FOR ITERATIVE DEBLENDING BY MEDIAN FILTERING

WEI CHEN[1,2], JIANG YUAN[3], YANGKANG CHEN[4] and SHUWEI GAN[3]

[1] *Key Laboratory of Exploration Technology for Oil and Gas Resources of the Ministry of Education, Yangtze University, Wuhan, Hubei 430100, P.R. China.*
[2] *Hubei Cooperative Innovation Center of Unconventional Oil and Gas, Wuhan, Hubei 430100, P.R. China. chenwei2014@yangtzeu.edu.cn*
[3] *State Key Laboratory of Petroleum Resources and Prospecting, China University of Petroleum, Fuxue Road 18, Beijing 102200, P.R. China. yuanjiang1990@163.com*
[4] *Bureau of Economic Geology, John A. and Katherine G. Jackson School of Geosciences, The University of Texas at Austin, University Station, Box X, Austin, TX 78713, U.S.A.*

(Received April 27, 2016; revised version accepted November 20, 2016)

ABSTRACT

Chen, W., Yuan, J., Chen, Y. and Gan, S., 2017. Preparing the initial model for iterative deblending by median filtering. *Journal of Seismic Exploration*, 26: 25-47.

Simultaneous-source acquisition can obtain much faster acquisition with higher spatial sampling at the cost of obtaining highly noisy seismic records. While researchers are seeking specific direct imaging algorithms for attenuating the simultaneous-source interference during the migration process, deblending is still a preferable way to deal with simultaneous-source seismic data at the current stage. Removing blending noise while preserving as much useful signal as possible is thought to be the key in the deblending process. Previous study has shown that the median filtering (MF) can be used to effectively and efficiently separate the simultaneous-source seismic data in the common midpoint domain based on one-step filtering. In this paper, we investigate the application of MF in preparing the initial model in an inversion-based deblending framework. Our results show that the application of MF in a shaping regularized iterative deblending framework can effectively accelerate the convergence rate and improve the deblending performance in a limited number of iterations. We use three different synthetic examples and one field data example to demonstrate our proposed methodology.

KEY WORDS: simultaneous source, deblending, shaping regularized iterative inversion, median filtering (MF), initial model of deblending.

0963-0651/17/$5.00

INTRODUCTION

The purpose of simultaneous source acquisition (or sometimes called multisource acquisition) is to speed up the acquisition of a higher-density seismic record by firing more than one source at nearly the same time. The simultaneous source acquisition allows temporal or spatial overlap of seismic records, and thus can save numerous acquisition cost and increase data quality. The benefits of simultaneous-source acquisition are compromised by the intense interference between different sources (Berkhout, 2008). Because of its economic benefits and technical challenges, this technique has attracted the attention of researches in both industry and academia (Mahdad et al., 2011; Huo et al., 2012; Gan et al., 2016b). One way for solving the problem caused by interference is by first - separating and second - processing strategy (Chen et al., 2014b), which is also called deblending. Another way is by direct imaging and inversion of the blended data by attenuating the interference during inversion process (Xue et al., 2016b; Chen et al., 2015; Gan et al., 2016c). For deblending, many successful applications have been reported, which have made huge savings of acquisition cost (Abma et al., 2010; Zhang et al., 2013; Alexander et al., 2013; Manning and Ahmad, 2013). There have also been several successful applications of direct imaging onto synthetic data (Jiang and Abma, 2010; Xue et al., 2016b; Chen et al., 2015), however, seldom successful applications of direct imaging onto field data have been reported in the past decade. Thus, deblending is still the dominant way for dealing with simultaneous-source data.

Currently existing deblending method falls into two categories. The first is filtering-based method (Hampson et al., 2008; Huo et al., 2012), which treats the deblending problem simply as a noise attenuation problem. Because, though coherent in the common shot domain, the blending noise has been demonstrated to be incoherent in other domains, such as common receiver, common offset or common midpoint domain (Beasley, 2008; Berkhout, 2008). Thus all the conventional denoising algorithms can be used in the deblending process. Because of the better coherency of useful signals in common midpoint domain, Chen et al. (2014c) proposed to use common midpoint domain for deblending. Since the near-offset useful events follow the hyperbolic assumption and can be flattened using normal moveout (NMO) correction, a simple median filtering (MF) can be applied to the NMO corrected common-midpoint (CMP) gathers to attenuate blending noise. Chen (2015) proposed a type of MF with spatially varying window length. The space-varying median filter (SVMF) does not require the events to be flattened and is also better applied in midpoint domain. Huo et al. (2012) used a multidirectional vector median filter after resorting the data into common midpoint gathers. Kim et al. (2009) simulated a noise model from the data and then adaptively subtracted the modeled noise from the acquired data in the common-offset domain.

The second type of deblending approaches is based on inversion, which treats the deblending problem as an inversion problem, and because of the ill-posed property of the blending equation, some specific constraints have to be added (Wapenaar et al., 2012a,b). Akerberg et al. (2008) used sparsity constraints in the Radon domain to regularize the inversion. A sparsity constraint was also used by Abma et al. (2010) to minimize the energy of incoherent events presented in blended data. Bagaini et al. (2012) compared two separation techniques for the dithered slip-sweep (DSS) data using the sparse inversion method and f-x predictive filtering (Canales, 1984; Chen and Ma, 2014), and pointed out the advantage of the inversion-based methods over the filtering-based methods. In order to deal with the aliasing problem, Beasley et al. (2012) proposed the alternating projection method (APM), which chooses corrective projections to exploit data characteristics and is claimed to be less sensitive to aliasing than alternative approaches. Mahdad et al. (2011) proposed a coherence-based inversion approach to deblend the simultaneous-source data. The convergence properties and the algorithmic aspects of the method were discussed by Doulgeris et al. (2012) and Mahdad et al. (2012), respectively. Borselen et al. (2012) proposed to distribute all energy in the simultaneous shot records by reconstructing the individual shot records at their respective locations. However, most of the published methods will either cause heavy signal leakage or require large iterative computation. New efficient and robust deblending scheme is still demanded. Chen et al. (2014b) proposed a general iterative deblending framework via shaping regularization (Fomel, 2007a). The constraint for the ill-posed inversion problem is applied via the shaping operator.

Median filter (MF) is well-known for its ability in removing out spiky noise in seismic profile after NMO or with relatively flatter events. It has been successfully utilized in the deblending process (Chen et al., 2014c; Chen, 2015), based on the simple one-step filtering approach. However, the integration of MF with an iterative inversion-based deblending approach has been seldom investigated. Considering that the conventional inversion-based deblending approach is very expensive, e.g., seislet transform (Gan et al., 2016a), curvelet transform (Zu et al., 2016), and high-resolution Radon transform(Xue et al., 2016a), a limited number of iterations are affordable in the real processing workflow. Finding a well-constructed initial model for the inversion-based deblending process is crucial for the convergence rate and final deblending performance. In this paper, we investigate the performance of a superior initial model for the whole iterative inversion by preparing the input data with MF. Three synthetic examples with different complexities and one field data example show that the initial model prepared using MF can accelerate the convergence greatly and improve the final deblending performance within a small number of iterations.

THEORY

Shaping regularized iterative deblending framework

According to Chen et al. (2014b), the deblending problem can be formulated as a basic estimation problem:

$$\mathbf{Fm} = \tilde{\mathbf{d}} \ , \tag{1}$$

where

$$\tilde{\mathbf{d}} = \begin{bmatrix} \mathbf{d} \\ \mathbf{T}^{-1}\mathbf{d} \end{bmatrix} , \quad \mathbf{F} = \begin{bmatrix} \mathbf{I} & \mathbf{T} \\ \mathbf{T}^{-1} & \mathbf{I} \end{bmatrix} , \quad \mathbf{m} = \begin{bmatrix} \mathbf{d}_1 \\ \mathbf{d}_2 \end{bmatrix} . \tag{2}$$

$\mathbf{d}_1$ and $\mathbf{d}_2$ denote the two unblended common receiver gathers, which are collected from a ocean bottom node (OBN) survey. $\mathbf{d}$ and $\mathbf{T}^{-1}\mathbf{d}$ denote the two blended common receiver gathers. There will be strong interference in the blended data due to simultaneous shooting of multiple sources. $\mathbf{I}$ is an identity operator. $\mathbf{T}$ and $\mathbf{T}^{-1}$ denote the forward and inverse dither operators (Chen et al., 2014b) or blending operators (Berkhout, 2008). The exact formulation of the dithering operator is given as follows:

$$\mathbf{T} = F^{-1}\mathbf{P}F \ , \tag{3}$$

where F and F^{-1} are forward and inverse Fourier transforms, respectively, and $\mathbf{P}$ is a N×N diagonal block phase-shift operator given by

$$\mathbf{P} = \begin{bmatrix} \mathbf{P}_1 & & & & & \\ & \mathbf{P}_2 & & & & \\ & & \mathbf{P}_3 & & & \\ & & & \ddots & & \\ & & & & \ddots & \\ & & & & & \mathbf{P}_n \end{bmatrix}_{N\times N} , \tag{4}$$

where $\mathbf{P}_n$ denotes the individual phase shift operator for n-th trace and can be expressed as a M × M diagonal matrix:

$$\mathbf{P}_n = \begin{bmatrix} e^{-i\omega\delta t_n} & & & & & \\ & e^{-i\omega\delta t_n} & & & & \\ & & e^{-i\omega\delta t_n} & & & \\ & & & \ddots & & \\ & & & & \ddots & \\ & & & & & e^{-i\omega\delta t_n} \end{bmatrix}_{M\times M} . \tag{5}$$

Here, ω denotes the angular frequency, δt_n denotes the random dithering time of the n-th trace. Series $\{\delta t_n\}$ is also called the dithering sequence or shot scheduling (Abma, 2014). M and N in eqs. (4) and (5) denote the number of temporal samples and number of traces, respectively.

An estimation of the model $\mathbf{m}$ can be iteratively obtained as follows:

$$\mathbf{m}_{n+1} = \mathbf{m}_n + \mathbf{B}\tilde{\mathbf{d}} - \mathbf{B}\mathbf{F}\mathbf{m}_n \ , \tag{6}$$

where $\mathbf{B}$ is the backward operator that provides an inverse mapping from data space to model space. If $\mathbf{B}$ is taken as the adjoint of $\mathbf{F}$, iteration (6) is known as the *Landweber iteration* (Landweber, 1951). The Landweber iteration solves the system of normal equations and converges to the least-squares estimate of $\mathbf{m}$:

$$\min_{\mathbf{m}} \| \mathbf{F}\mathbf{m} - \tilde{\mathbf{d}} \|_2^2 \ , \tag{7}$$

where $\| \cdot \|_2^2$ denotes the squared L_2 norm of a function. The least-squares optimization problem (7) is usually regularized by adding a regularization term:

$$\min_{\mathbf{m}} \| \mathbf{F}\mathbf{m} - \tilde{\mathbf{d}} \|_2^2 + \mathbf{R}(\mathbf{m}) \ , \tag{8}$$

where $\mathbf{R}(\cdot)$ is a regularization function. Alternatively, with a shaping operator $\mathbf{S}$ (Fomel, 2008), iteration (6) can be modified to the following equation:

$$\mathbf{m}_{n+1} = \mathbf{S}[\mathbf{m}_n + \mathbf{B}(\tilde{\mathbf{d}} - \mathbf{F}\mathbf{m}_n)] \ . \tag{9}$$

Regularized iteration (9) shapes the estimated model into the space of admissible models at each iterations (Fomel, 2007b, 2008). It has been proved that if $\mathbf{S}$ is a nonlinear thresholding operator (Donoho and Johnstone, 1994), $\mathbf{B} = \mathbf{F}^T$ where $\mathbf{F}^T$ is the adjoint operator of $\mathbf{F}$, iteration (9) converges to the solution of problem (8) with L_1 regularization term (Daubechies et al., 2004). A better choice for $\mathbf{B}$ is the pseudoinverse of $\mathbf{F}$: $\mathbf{B} = (\mathbf{F}^T\mathbf{F})^{-1}\mathbf{F}^T$ (Daubechies et al., 2008).

It has been proved that the pseudoinverse of the forward operator $\mathbf{F}$ is half of the identity operator when the random dithering range is small, which means that the optimal choice for the backward operator is $\mathbf{B} = (1/2)\mathbf{I}$. The Appendix gives a brief derivation to derive the pseudo-inverse of the forward operator. The shaping operator can be chosen either as a coherency promoting operator or as a sparsity promoting operator. In this paper, we use the seislet domain soft thresholding as the shaping operator. Thus, the minimization problem to be solved in this paper is as follows:

$$\hat{\mathbf{m}} = \arg\min_{\mathbf{m}} \| \mathbf{Fm} - \tilde{\mathbf{d}} \|_2^2 + \varepsilon^2 \| \mathbf{m} \|_1 \ , \tag{10}$$

where $\| \cdot \|_1$ denotes the L_1 norm of an input vector, ε^2 denotes a balancing parameter that compromise the data misfit term $\| \mathbf{Fm} - \tilde{\mathbf{d}} \|_2^2$ and the model sparsity term $\| \mathbf{m} \|_1$.

Median filter

Conventional MF is based on a scalar-value sorting process. When a set of scalars is sorted to be an ascending or descending sequence, the middle value is chosen to stand for this sequence. In signal-processing or geophysical data analysis fields, this filter is commonly used to remove spiky noise. The more general mathematical formulation of a MF is given as:

$$\hat{u}_i = \arg\min_{u_m \in S_i} \sum_{l=1}^{L} \| u_m - u_l \|_p \ , \tag{11}$$

where $\hat{u}_i$ is the output value for location x_i, $S_i = \{u_1, u_2, \ldots, u_L\}$. It's worth to be mentioned that in eq. (11), i is the position index in a 1D sequence, l and m are both indices in the filtering window. L is the length of the filtering window and p denotes the L_p norm. Commonly $p = 1$ corresponds to a standard MF. The classic MF has been utilized by Chen et al. (2014c) for separating simultaneous sources based on one-step filtering in the NMO corrected CMP gathers.

Preparing the initial model by median filtering

The special "spiky" feature of blending noise provides a suitable application for the conventional MF. In a common offset domain, where useful events are mainly flat and blending noise is incoherent along the spatial direction, a MF can adequately remove out those noise. In some other domains, the MF can not only remove the blending noise but also remove some useful signals. In this case, we propose to use the MF as a preprocessing tool, and we treat the MF filtered data as the initial model to the subsequent iterative framework to get a faster convergence. The lost useful signal, however, can be recovered during the subsequent iterative inversion. Note that the initial model used in the conventional framework is usually zero. Fig. 1 demonstrates how median filter can be implemented into a common deblending framework. As we can see in the flowchart, in ideal cases, an acceptable result might be obtained only through a median filtering process. If we are more strict to the result, we

can utilize iterative inversion to obtain a better deblending performance. Preparing the initial model by MF can not only accelerate the convergence, but also will improve the final deblending performance. Since many sparse transforms are not exactly invertible, such as the seislet transform, high-resolution radon transform, we can not afford too many iterations, otherwise we will introduce extra error due to the transform itself. In the following section, we will use different type of examples to show the advantage of applying MF for preparing the initial model.

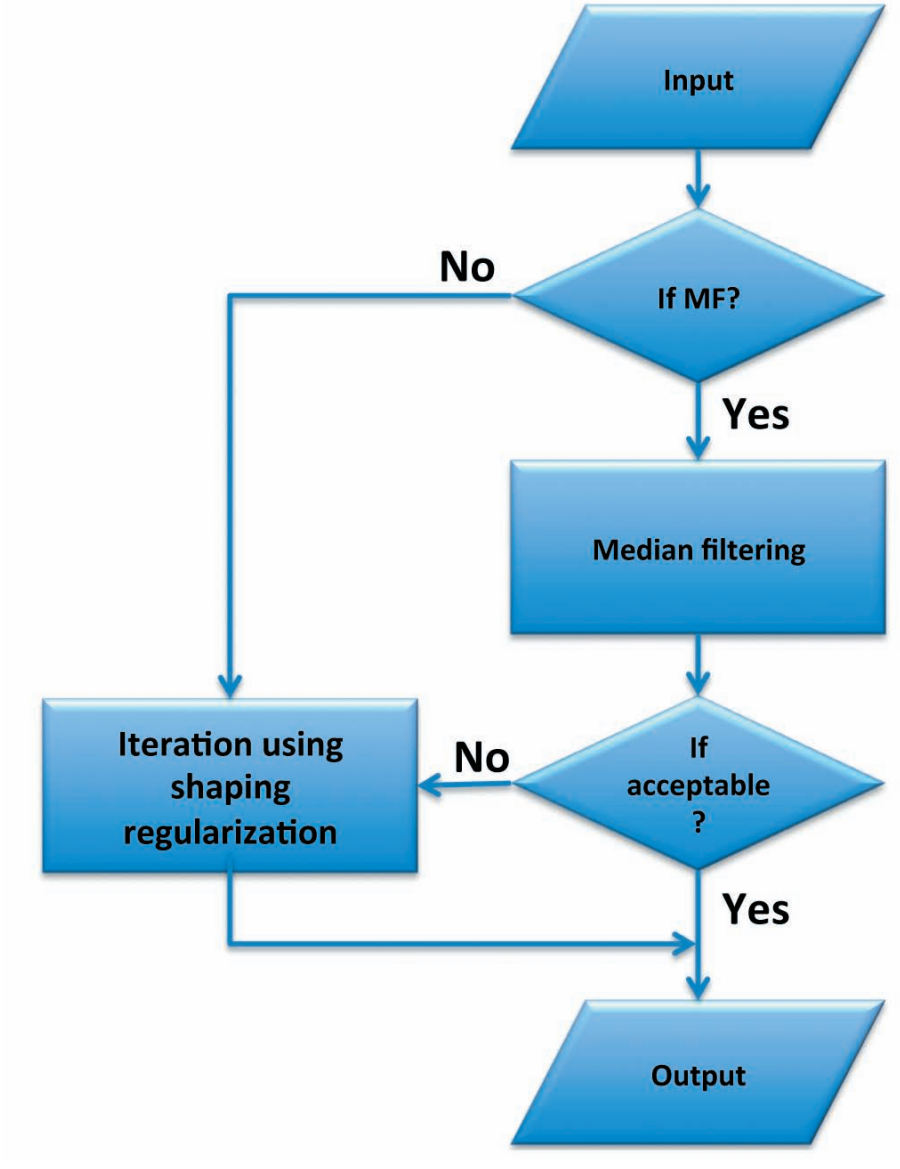

Fig. 1. Workflow of using median filter to prepare the initial model for deblending.

EXAMPLES

We use three different synthetic datasets and one field dataset to test the effect of median filter (MF) as a preprocessing step in the whole deblending process. The first and third examples can be used to demonstrate the deblending performance in common offset domain, the second synthetic example and field example can be used to demonstrate the deblending performance in common receiver domain. In all the example, we blended data using the random dithering method introduced in Chen et al. (2014b). The source and receiver geometry is shown in Fig. 2. The dots denote different shots for two different sources. The inverted triangles denote the constant receivers. Because of the symmetry of the two sources, we only show the deblending performance for one source. The two arrows denote the sailing directions of two sources. In this paper, both sources sail from the west towards the east.

In order to test the convergence rate, we apply SNR (Chen et al., 2014a) as the measurement of deblending performance in the following form:

$$\mathrm{SNR} = 10\log_{10}(\|\mathbf{d}\|_2^2/\|\mathbf{d} - \tilde{\mathbf{d}}\|_2^2) \quad , \tag{12}$$

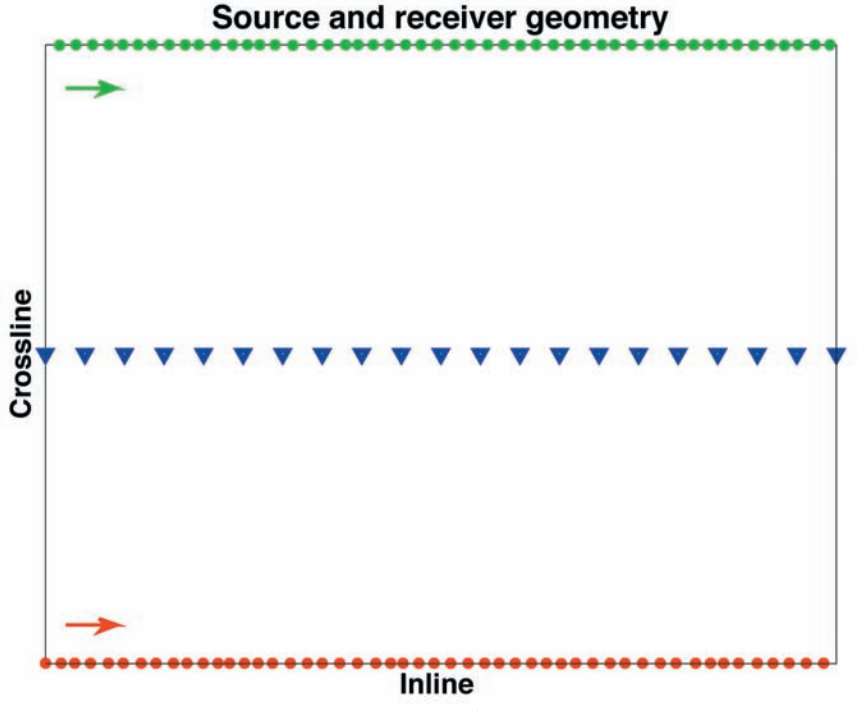

Fig. 2. Demonstration of the source and receiver geometry for the blended acquisition used in the presented four examples.

where $\tilde{\mathbf{d}}$ denotes the deblended data, $\mathbf{d}$ denotes the unblended data and the unit of SNR is dB.

The first example is a flat-event example, as shown in Fig. 3. The traditionally acquired clean unblended data is shown in Fig. 3a. The blended data is shown in Fig. 3b.

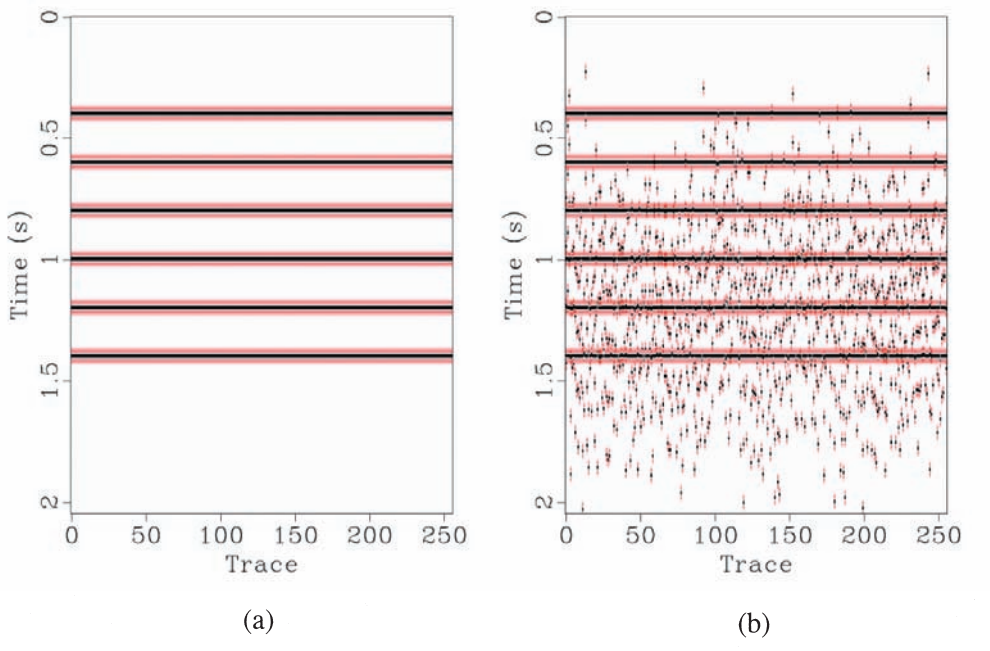

Fig. 3. First synthetic example (sorted to common offset domain). (a) Unblended data. (b) Blended data.

In this example, applying a MF onto the blended data obtains a nearly perfect estimation (see Fig. 4a). We can use the result as an initial model for the subsequent iterative framework, thus we can get a more precise estimation. The result using MF and MF embedded iterative framework do not have much difference. However, if we do not use MF as a preprocessing tool, the iteration is much slower (see Fig. 5).

The second synthetic example is a linear-events example. The clean unblended and noisy blended data are shown in Figs. 6a and 6b, respectively. The MF also does a good job for the second synthetic example, as shown in Fig. 7a. Even though there exists some coherent energy in the noise section and error section, considering that the amplitude of the coherent part is actually very

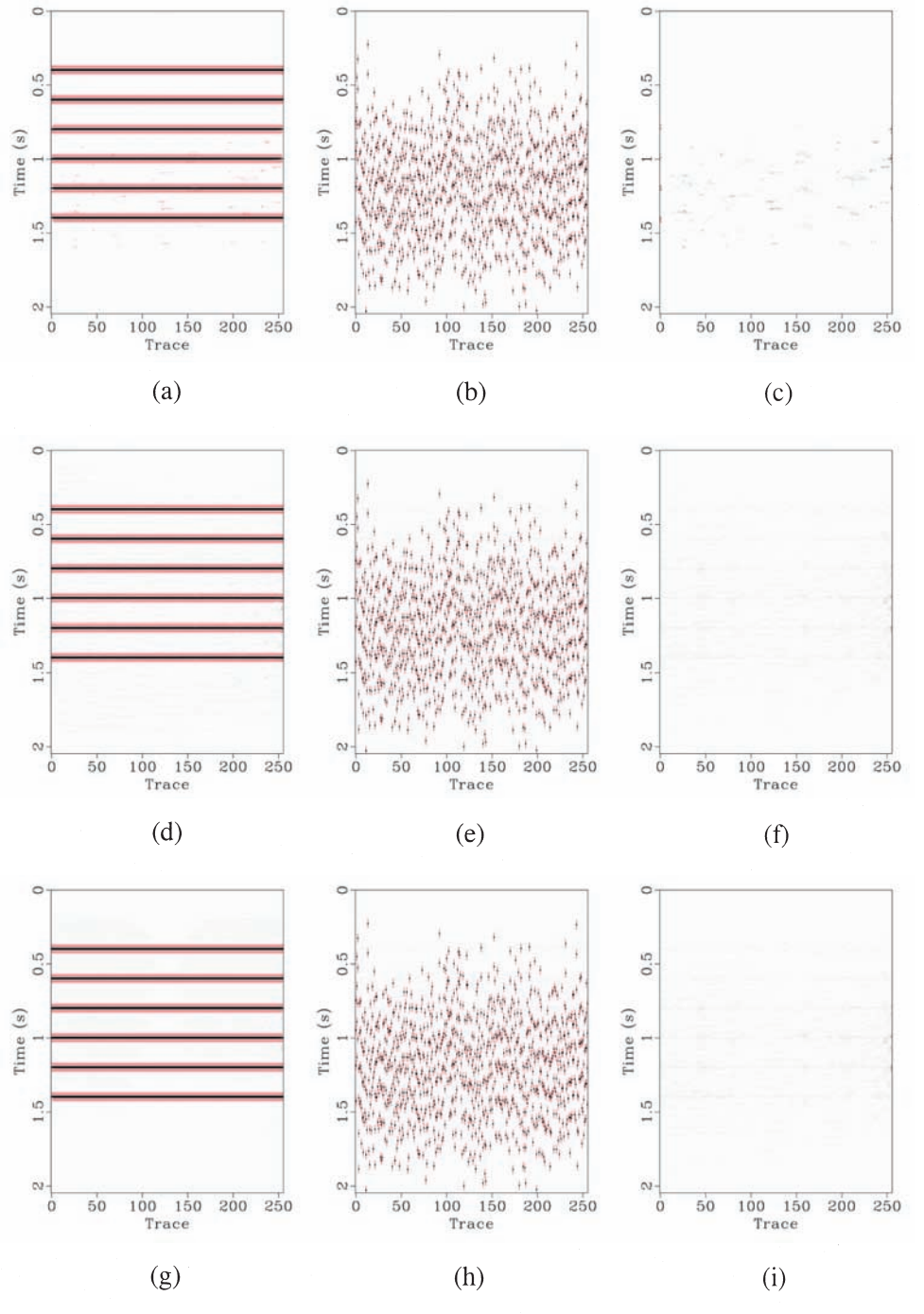

Fig. 4. Deblending results comparison for the first synthetic example. (a) Deblending result using MF. (b) Blending noise corresponding to (a). (c) Error section corresponding to (a). (d)-(f) Deblending using shaping regularized iterative framework. (g)-(i) Deblending using the proposed approach.

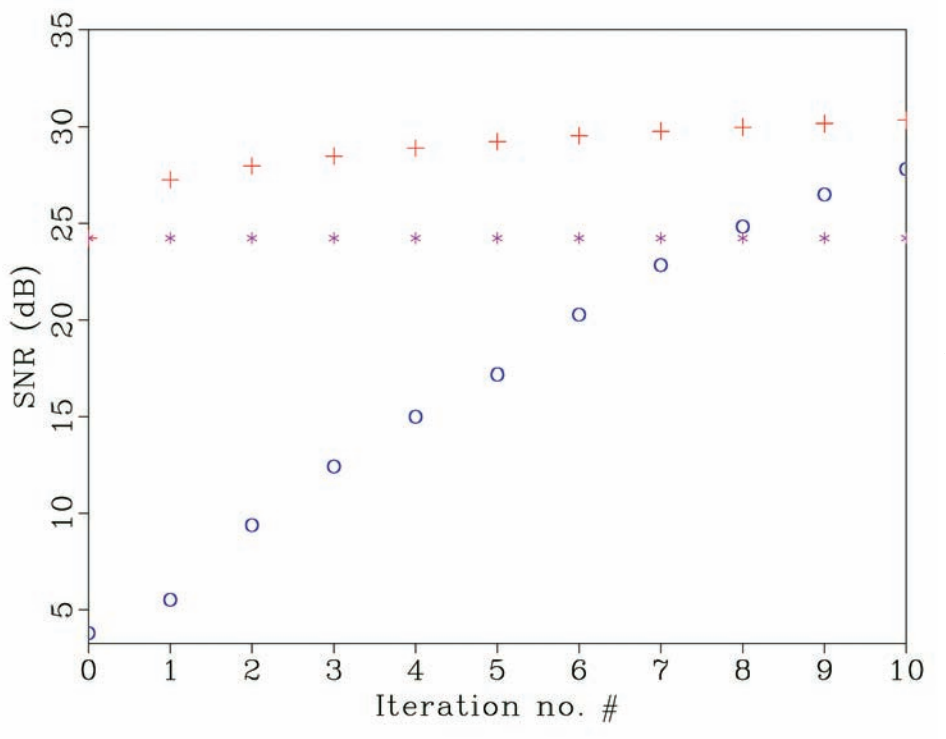

Fig. 5. SNR diagrams for the first synthetic example. The "+" line corresponds to the proposed approach. The "*" line corresponds to deblending using MF. The "o" line corresponds to the shaping regularized iterative framework.

small and the process is done in one step without any other procedures, this result is still acceptable, especially when a quick look at the deblending result or the subsequent migration result is needed. Here, difference section denotes the difference between the deblended data and the blended data) and error section denotes the difference between the deblended data and the original unblended data. Furthermore, we can treat it as the initial model for the subsequent iterative estimation, and then we can get a perfect estimation with a faster convergence (see Fig. 8).

The third example is a very complicated synthetic example, which contains not only useful hyperbolic reflection events, but also unwanted dipping interference and ground roll noise. The clean unblended and noisy blended data are shown in Fig. 9. In this example, the one-step MF does not enjoy much benefit, because using MF harms much of the useful energy, as shown in Figs. 10a-10c. According to the SNR diagrams, using a MF embedded iterative framework enjoys a faster convergence, which demonstrate the advantage of MF

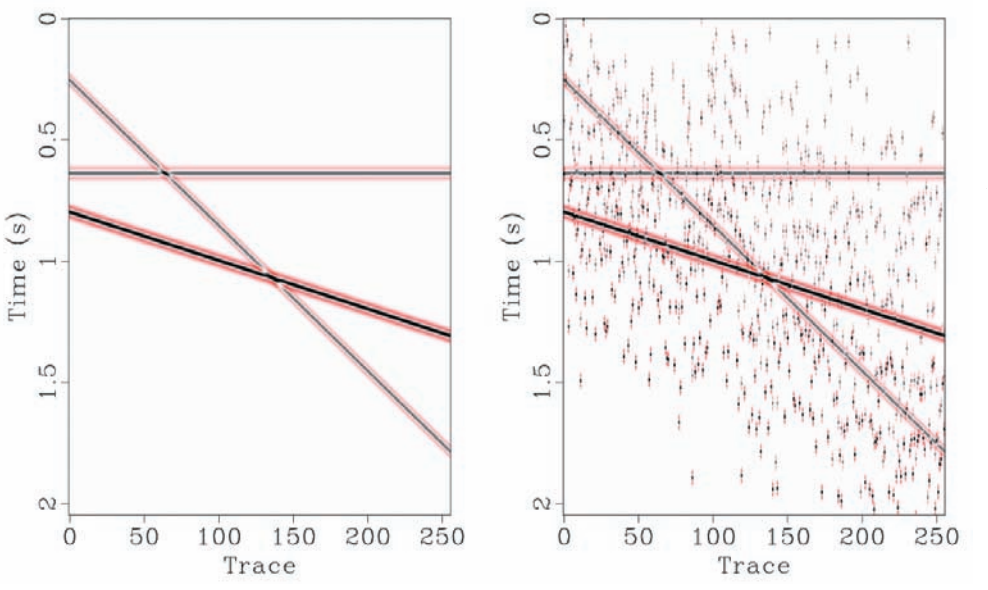

Fig. 6. Second synthetic example (sorted to common offset domain). (a) Unblended data. (b) Blended data.

as a preprocessing tool. The deblending performance for the field data example is shown in Fig. 13. The deblending performance is much similar to the deblending performance of the third synthetic example. Although the sole MF will cause some damage to the useful energy, the subsequent iterative inversion based on this initial model will compensate for the energy loss in MF. The MF embedded iterative inversion can also obtain a much better deblending result compared with that from the traditional iterative inversion without the preprocessed initial model. The error section using the proposed approach is nearly zero across the whole profile while the traditional approach still cause some visible error. The convergence diagrams using three different approaches are shown in Fig. 14. The comparison confirms that the proposed approach can obtain faster convergence and better deblended result.

In order to show how the blending interference looks like in different domains and how the proposed method help attenuating the interference in a clearer way, we show the whole field data set before and after deblending in Fig. 15. Fig. 15a shows the unblended data. Please note that the two spatial dimensions are "shot" and "receiver". Fig. 15b shows the blended data. It is obvious that in each common receiver gather, the interference is incoherent due

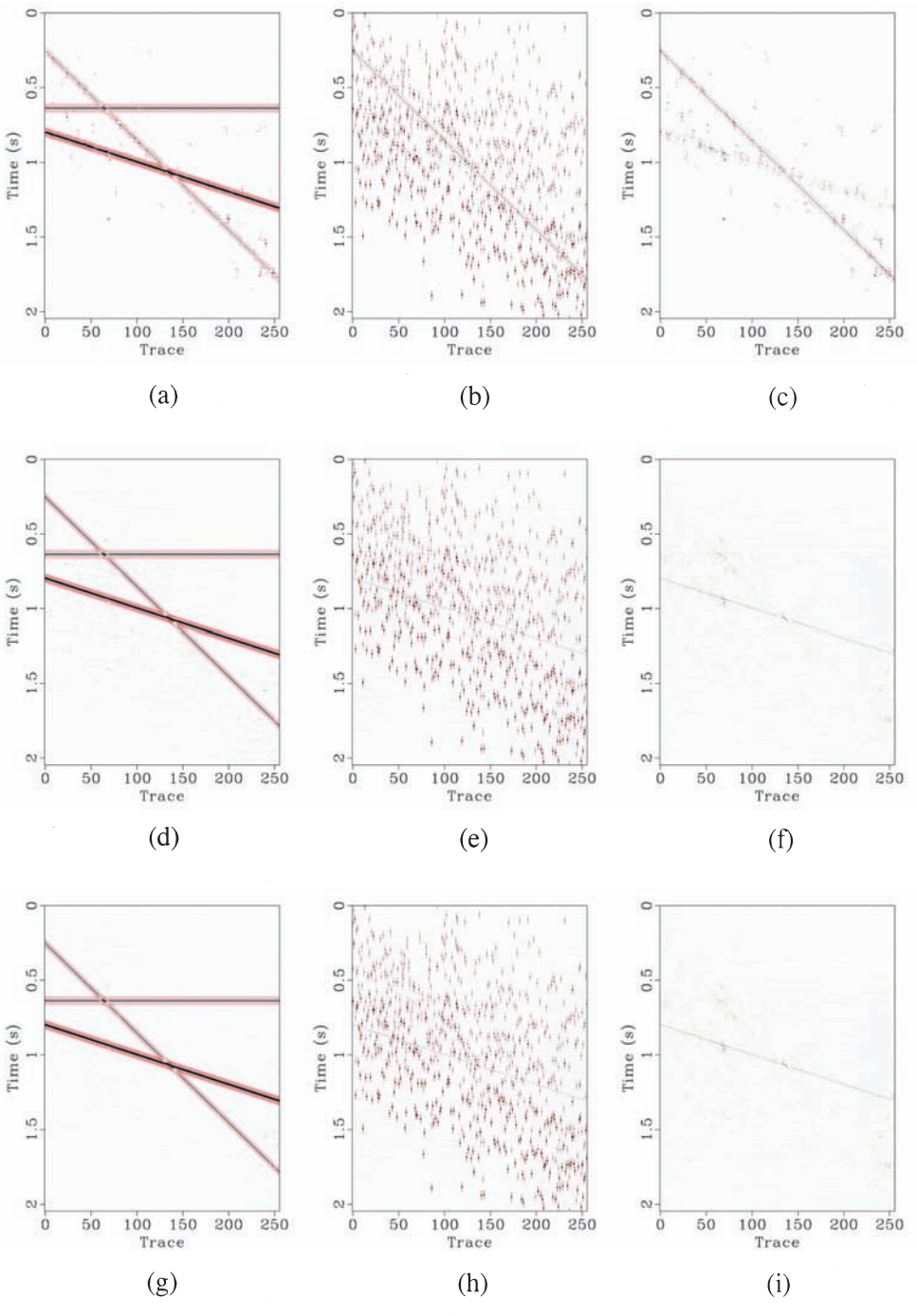

Fig. 7. Deblending results comparison for the second synthetic example. (a) Deblending result using MF. (b) Blending noise corresponding to (a). (c) Error section corresponding to (a). (d)-(f) Deblending using shaping regularized iterative framework. (g)-(i) Deblending using the proposed approach.

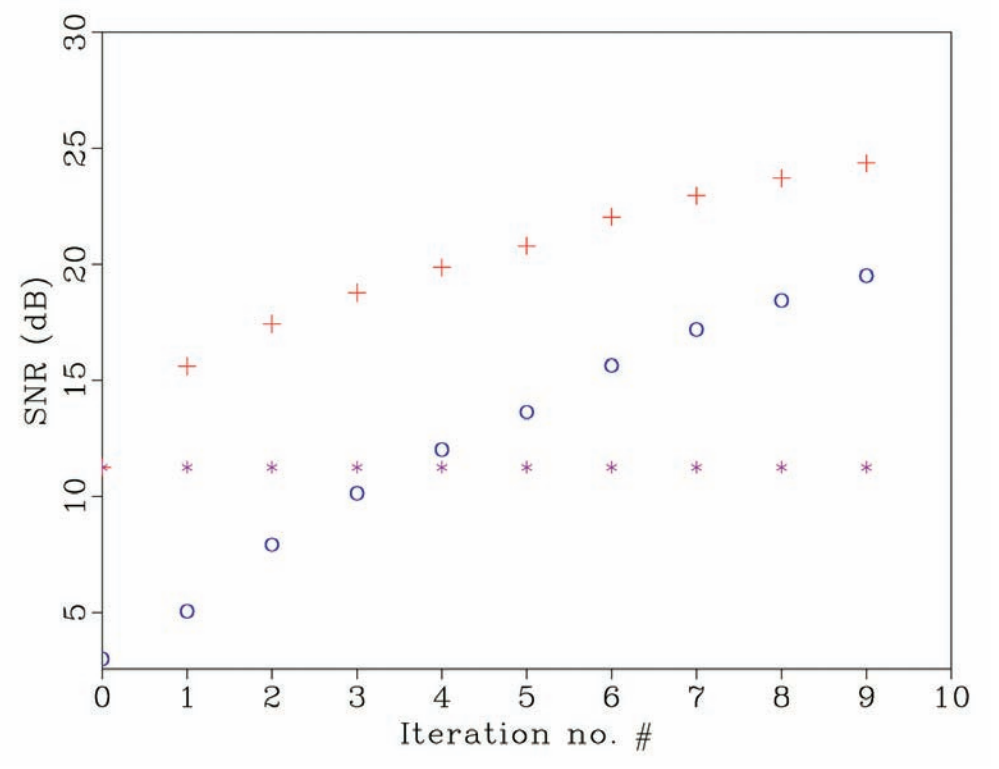

Fig. 8. SNR diagrams for the second synthetic example. The "+" line corresponds to the proposed approach. The "*" line corresponds to deblending using MF. The "o" line corresponds to the shaping regularized iterative framework.

to the random shot scheduling. However, in each common shot gather, the interference is coherent. It also demonstrate the reason why we need to apply the proposed method in common receiver gather. After using the proposed approach, the deblended data is shown in Fig. 15c. Both coherent and incoherent interference that is shown in Fig. 15b has been removed in Fig. 15c. Fig. 15d shows the difference between the deblended data and blended data. The energy in common receiver gather is incoherent and shows that the proposed method does not damage any useful coherent signals.

DISCUSSIONS AND CONCLUSIONS

The ability of MF to attenuate high-amplitude spiky noise is nearly irreplaceable. Although strictly the blending noise is rather wavelet-like than spike-like noise, the high-amplitude peaks appear similar to spiky noise along the spatial dimension. Thus they can be removed out by MF while leaving the

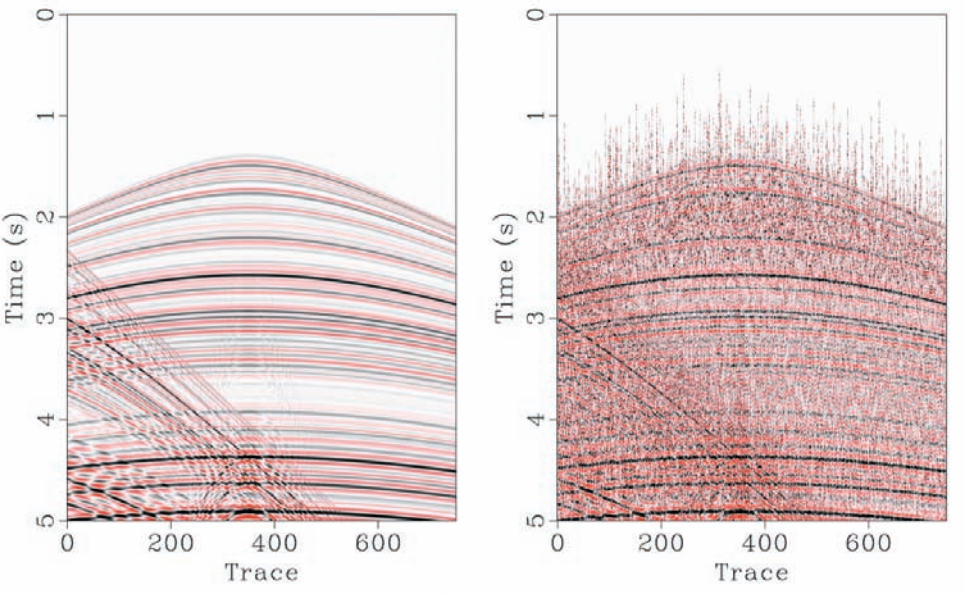

Fig. 9. Third synthetic example (sorted to common receiver domain). (a) Unblended data. (b) Blended data.

small-amplitude parts to be filtered by some other effective filters like f-x deconvolution or f-k filter (Mahdad et al., 2012). For simpler seismic profiles, utilizing a MF alone is adequately to fulfill the requirements (e.g., Fig. 4a). For more realistic complicated profiles, MF can be used to prepare the superior initial model, which can make the subsequent iterative inversion faster converged and more stable. The proposed framework simply uses a classic version of MF, and can be widely used in different research or industry environment. Utilizing more sophisticated version of MF to better prepare the initial model is worth being investigated, which is the ongoing project.

Finding a well-constructed initial model for the iterative inversion based deblending is crucial for the convergence rate and final deblending performance. In the paper, we investigate the impact of a superior initial model after median filtering on the whole iterative inversion. Three synthetic examples with different complexities and one field data example show that the initial model prepared using MF can accelerate the convergence greatly and improve the final deblending performance within a small number of iterations. While the initial MF will cause some damage to the useful energy, the lost energy will be compensated during the subsequent iterative iterations. The improvement of the proposed approach is due to the anti-spike ability of a traditional MF.

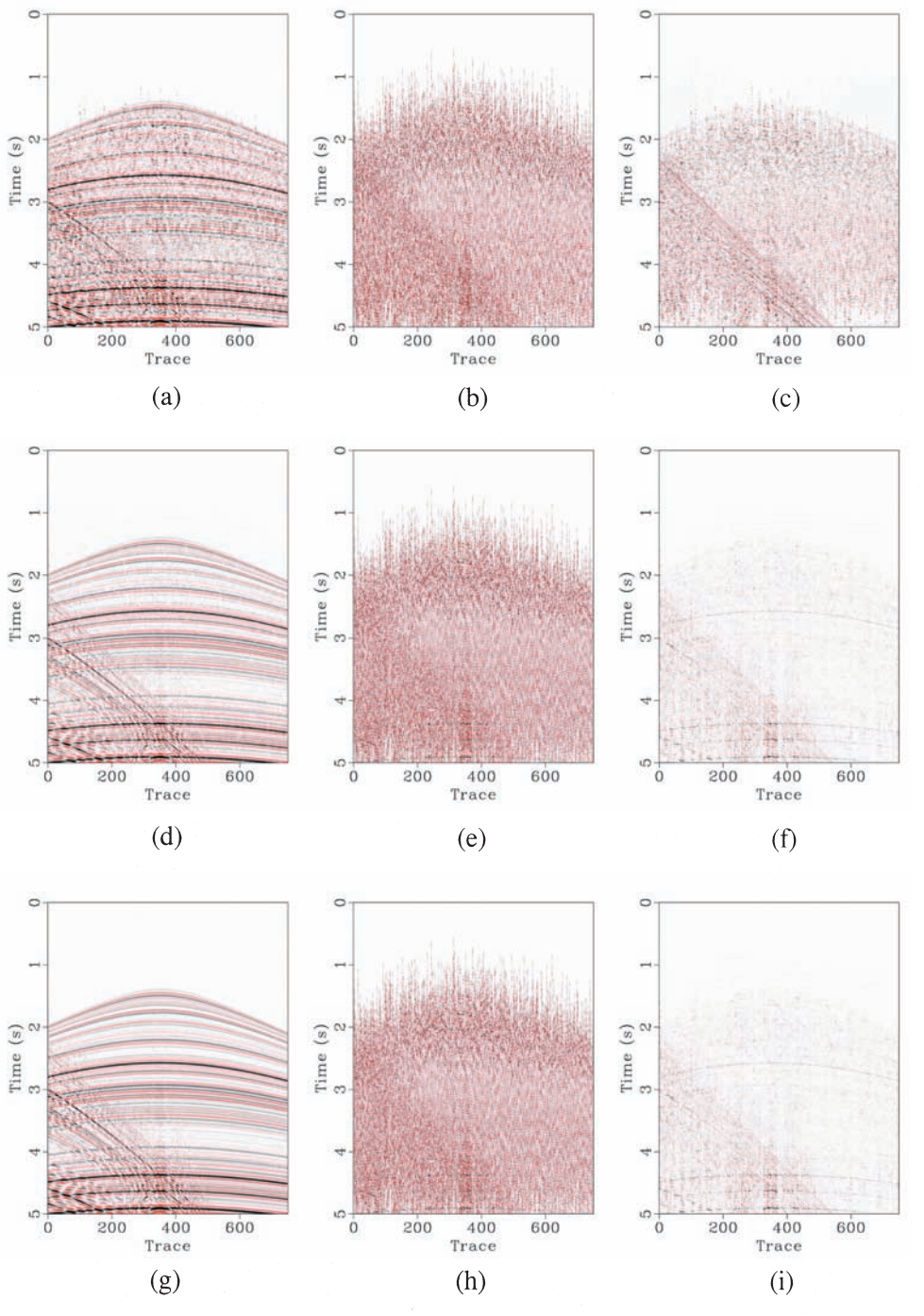

Fig. 10. Deblending results comparison for the third synthetic example. (a) Deblending result using MF. (b) Blending noise corresponding to (a). (c) Error section corresponding to (a). (d)-(f) Deblending using shaping regularized iterative framework. (g)-(i) Deblending using the proposed approach.

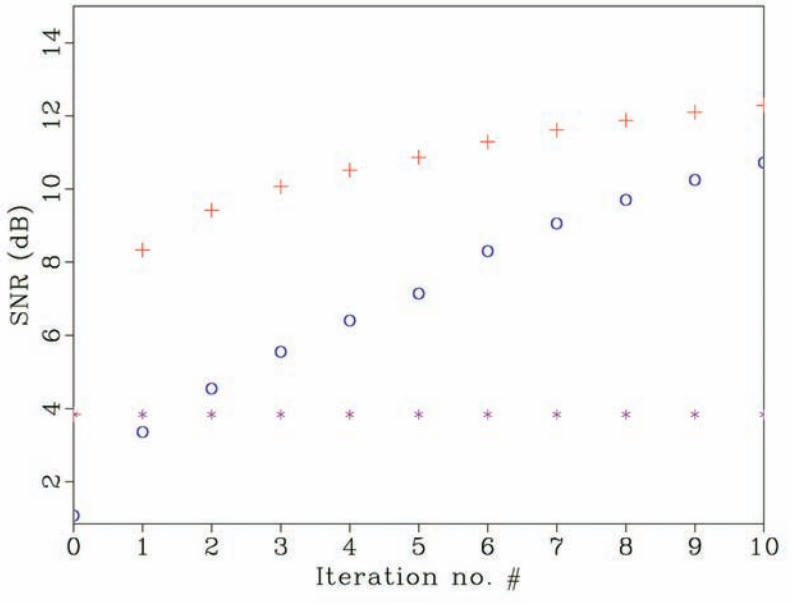

Fig. 11. SNR diagrams for the third synthetic example. The "+" line corresponds to the proposed approach. The "*" line corresponds to deblending using MF. The "o" line corresponds to the shaping regularized iterative framework.

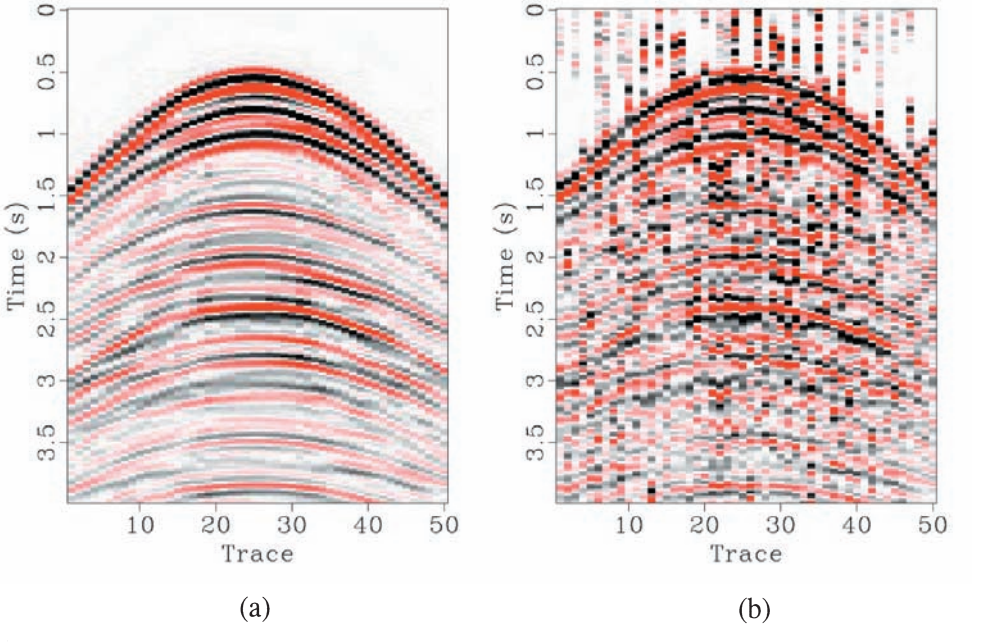

Fig. 12. Field data example (sorted to common receiver domain). (a) Unblended data. (b) Blended data.

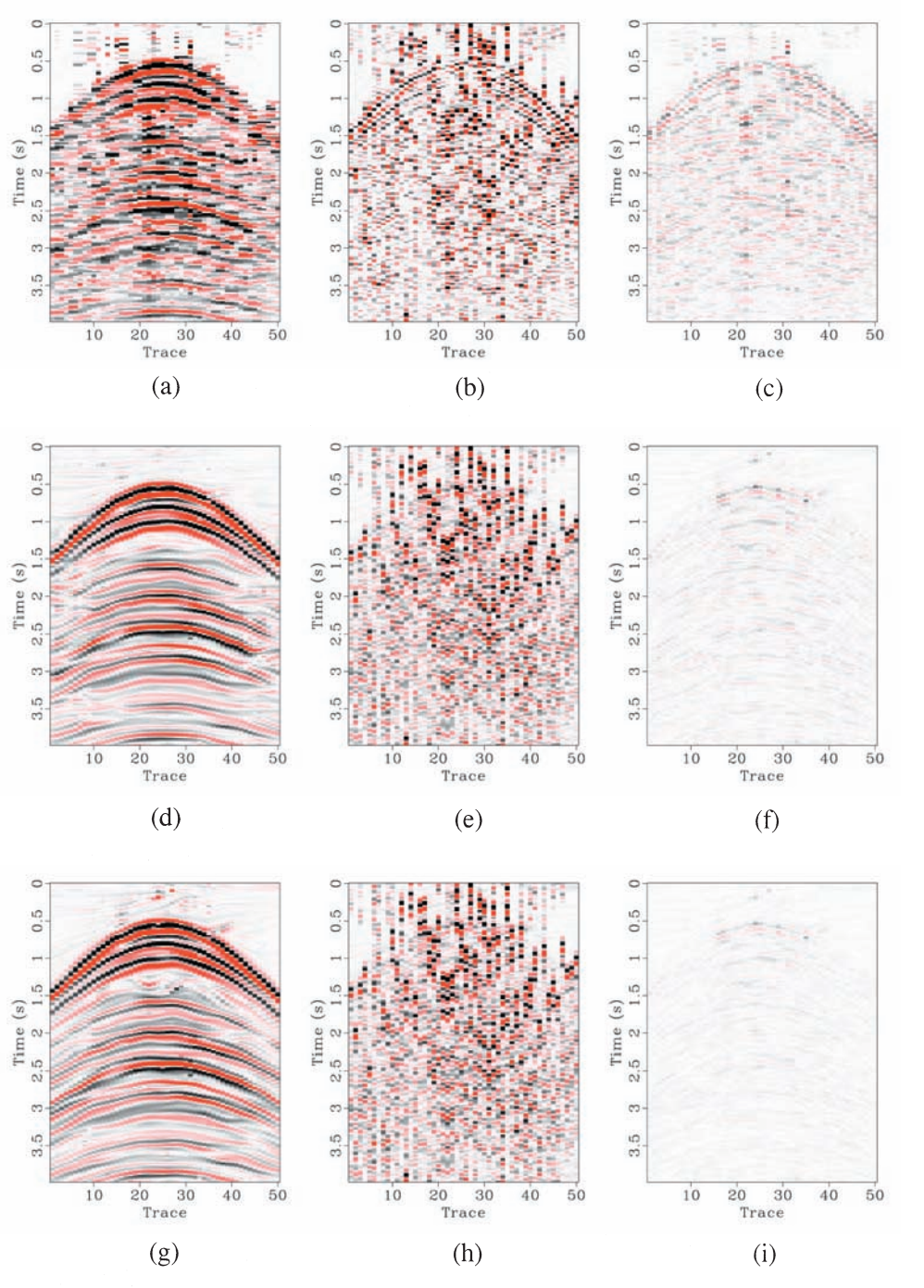

Fig. 13. Deblending results comparison for the field data example. (a) Deblending result using MF. (b) Blending noise corresponding to (a). (c) Error section corresponding to (a). (d)-(f) Deblending using shaping regularized iterative framework. (g)-(i) Deblending using the proposed approach.

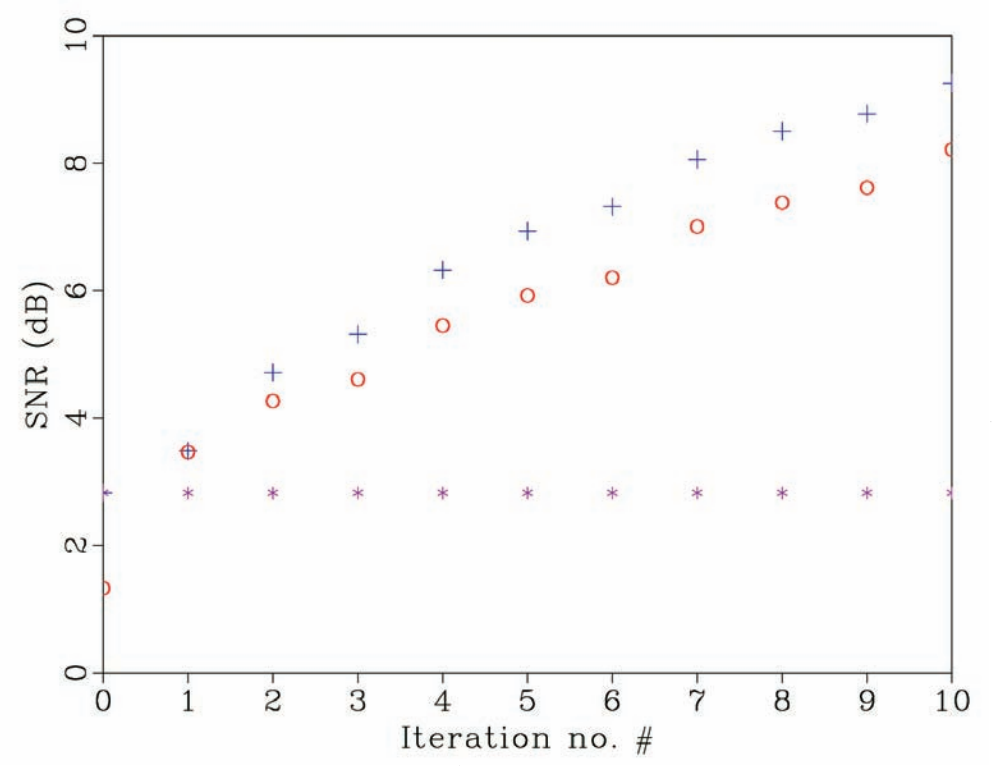

Fig. 14. SNR diagrams for the field data example. The "+" line corresponds to the proposed approach. The "*" line corresponds to deblending using MF. The "o" line corresponds to the shaping regularized iterative framework.

ACKNOWLEDGMENTS

We would like to thank Josef Paffenholz, Araz Mahdad, Ray Abma, Min Zhou, Qie Zhang, Zhiyong Jiang, Shan Qu, Shaohuan Zu, Zhaoyu Jin, Lele Zhang for inspiring discussions and helpful suggestions. Yangkang Chen would like to thank FairfieldNodal and BP America for providing the opportunity for two summer internships in the study of simultaneous source separation. This work is partially supported by Texas Consortium for Computational Seismology (TCCS) and Sinopec Key Laboratory of Geophysics (Grant No. 33550006-15-FW2099-0017).

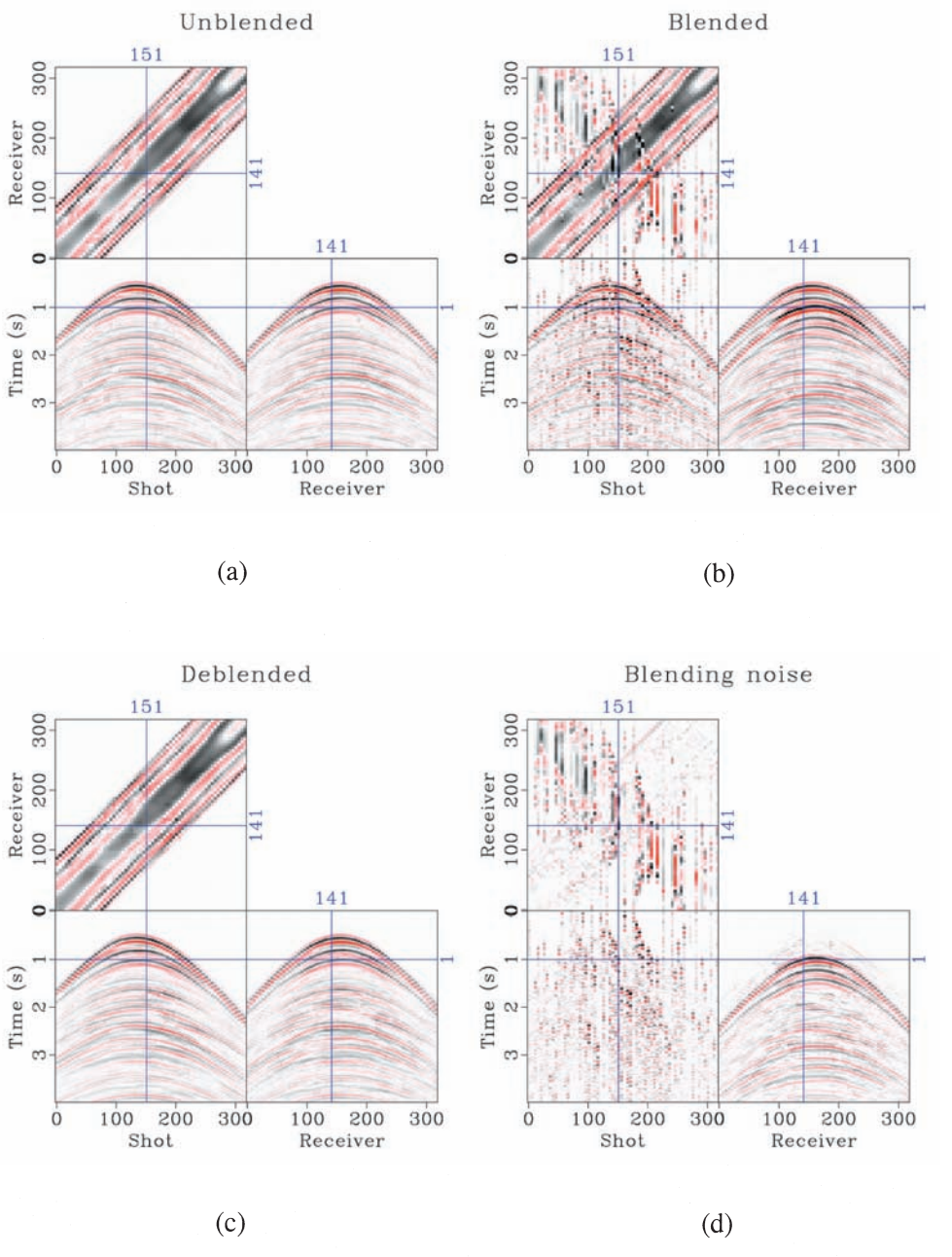

Fig. 15. Deblending results for all common receiver gathers. (a) Unblended data. (b) Blended data. (c) Deblended data using the proposed method. (d) Removed blending interference. Note that the interference appears incoherent in common receiver gather but coherent in common shot domain. The unblended and deblended data are almost the same, which confirms the effectiveness of the proposed method.

REFERENCES

Abma, R.L., 2014. Shot scheduling in simultaneous shooting. Expanded Abstr., 84th Ann. Internat. SEG Mtg., Denver: 94-98.

Abma, R.L., Manning, T., Tanis, M., Yu, J. and Foster, M., 2010. High quality separation of simultaneous sources by sparse inversion. Extended Abstr., 72nd EAGE Conf., Barcelona.

Akerberg, P., Hampson, G., Rickett, J., Martin, H. and Cole, J., 2008. Simultaneous source separation by sparse radon transform. Expanded Abstr., 78th Ann. Internat. SEG Mtg., Las Vegas: 2801-2805.

Alexander, G., Abma, R., Clarke, R. and Dart, S.L., 2013, Processing results of simultaneous source surveys compared to conventional surveys. Expanded Abstr., 83rd Ann. Internat. SEG Mtg., Houston: 104-108.

Bagaini, C., Daly, M. and Moore, I., 2012. The acquisition and processing of dithered slip-sweep vibroseis data. Geophys. Prosp., 60: 618-639.

Beasley, C.J., 2008. A new look at marine simultaneous sources. The Leading Edge, 27: 914-917.

Beasley, C.J., Dragoset, B. and Salama, A., 2012. A 3D simultaneous source field test processed using alternating projections: a new active separation method. Geophys. Prosp., 60: 591-601.

Berkhout, A.J., 2008. Changing the mindset in seismic data acquisition. The Leading Edge, 27: 924-938.

Borselen, R.V., Baardman, R., Martin, T., Goswami, B. and Fromyr, E., 2012. An inversion approach to separating sources in marine simultaneous shooting acquisition-application to a Gulf of Mexico data set. Geophys. Prosp., 60: 640-647.

Canales, L., 1984. Random noise reduction. Expanded Abstr., 54th Ann. Internat. SEG Mtg. Atlanta: 525-527.

Chen, Y., 2015. Deblending using a space-varying median filter. Explor. Geophys., 46: 332-341.

Chen, Y., Zhou, C., Yuan, J. and Jin, Z., 2014a. Application of empirical mode decomposition to random noise attenuation of seismic data. J. Seismic Explor., 23: 481-495.

Chen, Y., Fomel, S. and Hu, J., 2014b. Iterative deblending of simultaneous-source seismic data using seislet-domain shaping regularization. Geophysics, 79: V179-V189.

Chen, Y. and Ma, J., 2014, Random noise attenuation by f-x empirical mode decomposition predictive filtering. Geophysics, 79: V81-V91.

Chen, Y., Yuan, J., Jin, Z., Chen, K. and Zhang, L., 2014c. Deblending using normal moveout and median filtering in common-midpoint gathers. J. Geophys. Engineer., 11(4): 045012.

Chen, Y., Yuan, J., Zu, S., Qu, S. and Gan, S., 2015. Seismic imaging of simultaneous-source data using constrained least-squares reverse time migration. J. Appl. Geophys., 114: 32-35.

Daubechies, I., Defrise, M. and Mol, C.D., 2004. An iterative thresholding algorithm for linear inverse problems with a sparsity constraint. Communicat. Pure Appl. Mathemat., 57: 1413-1457.

Daubechies, I., Fornasier, M. and Loris, I., 2008. Accelerated projected gradient method for linear inverse problems with sparsity constraints. J. Fourier Analys. Applicat., 14: 764-792.

Donoho, D.L. and Johnstone, I.M., 1994. Ideal spatial adaptation by wavelet shrinkage. Biometrika, 81: 425-455.

Doulgeris, P., Bube, K., Hampson, G. and Blacquière, G., 2012. Covergence analysis of a coherency-constrained inversion for the separation of blended data. Geophys. Prosp., 60: 769-781.

Fomel, S., 2007a. Shaping regularization in geophysical-estimation problems. Geophysics, 72: R29-R36.

Fomel, S., 2007b. Shaping regularization in geophysical-estimation problems. Geophysics, 72: R29-R36.

Fomel, S., 2008. Nonlinear shapping regularization in geophysical inverse problems. Expanded Abstr., 78th Ann. Internat. SEG Mtg., Las Vegas: 2046-2051.

Gan, S., Wang, S., Chen, Y. and Chen, X., 2016a. Simultaneous-source separation using iterative seislet-frame thresholding. IEEE Geosci. Remote Sens. Lett., 13: 197-201.

Gan, S., Wang, S., Chen, Y., Chen, X. and Xiang, K., 2016b. Separation of simultaneous sources using a structural-oriented median filter in the flattened dimension. Comput. Geosci., 86: 46-54.

Gan, S., Wang, S., Chen, Y., Qu, S. and Zu, S., 2016c. Velocity analysis of simultaneous- source data using high-resolution semblance coping with the strong noise. Geophys. J. Internat., 204: 768-779.

Hampson, G., Stefani, J. and Herkenhoff, F., 2008. Acquisition using simultaneous sources. The Leading Edge, 27: 918-923.

Huo, S., Luo, Y. and Kelamis, P.G., 2012. Simultaneous sources separation via multidirectional vector-median filtering. Geophysics, 77: V123-V131.

Jiang, Z. and Abma, R., 2010. An analysis on the simultaneous imaging of simultaneous source data. Expanded Abstr., 80th Ann. Internat. SEG Mtg., Denver: 3115-3118.

Kim, Y., Gruzinov, I., Guo, M. and Sen, S., 2009. Source separation of simultaneous source OBC data. Expanded Abstr., 79th Ann. Internat. SEG Mtg., Houston: 51-55.

Landweber, 1951. An iteration formula for Fredholm integral equations of the first kind. Am. J. Mathemat., 73: 615-624.

Mahdad, A., Doulgeris, P. and Blacquière, G., 2011. Separation of blended data by iterative

APPENDIX

PSEUDO-INVERSE OF THE FORWARD OPERATOR

In eq. (3), considering that the Fourier operator (with symmetric normalization) and the phase shift operator are both unitary, which means $F^{-1} = F^{\mathrm{T}}$ and $\mathbf{P}^{-1} = \mathbf{P}^{\mathrm{T}}$, it is easy to derive that

$$\mathbf{T}^{\mathrm{T}} = (F^{-1}\mathbf{P}F)^{\mathrm{T}} = F^{\mathrm{T}}\mathbf{P}^{\mathrm{T}}F = (F^{-1}\mathbf{P}F)^{-1} = \mathbf{T}^{-1} \quad . \tag{A-1}$$

Thus, the dithering operator is proven to be a unitary operator.

Furthermore,

$$\begin{aligned} \mathbf{F}^{T} &= \begin{bmatrix} \mathbf{I} & \mathbf{T} \\ \mathbf{T}^{-1} & \mathbf{I} \end{bmatrix}^{T} = \begin{bmatrix} \mathbf{I} & \mathbf{T}^{-T} \\ \mathbf{T}^{T} & \mathbf{I} \end{bmatrix} = \begin{bmatrix} \mathbf{I} & \mathbf{T} \\ \mathbf{T}^{-1} & \mathbf{I} \end{bmatrix} = \mathbf{F}, \\ \mathbf{F}^{T}\mathbf{F} &= \begin{bmatrix} \mathbf{I} & \mathbf{T} \\ \mathbf{T}^{-1} & \mathbf{I} \end{bmatrix} \begin{bmatrix} \mathbf{I} & \mathbf{T} \\ \mathbf{T}^{-1} & \mathbf{I} \end{bmatrix} = 2 \begin{bmatrix} \mathbf{I} & \mathbf{T} \\ \mathbf{T}^{-1} & \mathbf{I} \end{bmatrix} = 2\mathbf{F}. \end{aligned} \tag{A-2}$$

The pseudo-inverse of the forward operator is therefore:

$$\hat{\mathbf{m}} = (\mathbf{F}^{\mathrm{T}}\mathbf{F})^{-1}\mathbf{F}^{\mathrm{T}} = \tfrac{1}{2}\mathbf{F}^{-1}\mathbf{F}^{\mathrm{T}} = \tfrac{1}{2}\mathbf{I} \quad . \tag{A-3}$$